

BELLCOMM, INC.

1100 Seventeenth Street, N.W. Washington, D. C. 20036

SUBJECT: Structural Loads Induced by AAP
Spacecraft Docking Dynamics
Case 620

DATE: April 1, 1968

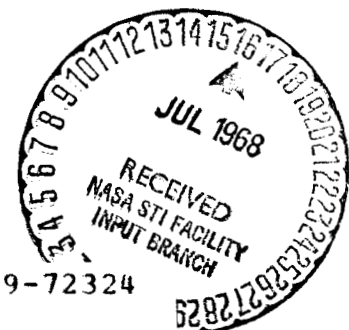
FROM: W. W. Hough

ABSTRACT

The bending-moment at the LM/MDA interface that occurs during the CSM axial docking maneuver has been analyzed in detail by MSC and Martin. Their results differ because of different mathematical models. The Martin analysis uses a LM/MDA interface stiffness model that is more flexible than the MSC model, and Martin's result for maximum bending moment is a factor-of-five less than MSC's.

In this memorandum, LM/MDA interface moment is examined as a function of interface stiffness using two analytic approaches and a simplified model. The conclusion that the bending moment can be reduced by lowering the interface stiffness is reached. MSFC and Martin have reached the same conclusion, but the Structures and Mechanics Division at MSC disagrees. MSC's objections are discussed.

(NASA-CR-95430) STRUCTURAL LOADS INDUCED BY
AAP SPACECRAFT DOCKING DYNAMICS (Bellcomm,
Inc.) 16 p



N79-72324

Unclas

00/18 11179

FF No.	(NASA CR OR TMX OR AD NUMBER)	(CATEGORY)
	[REDACTED]	

BELLCOMM, INC.

1100 Seventeenth Street, N.W. Washington, D. C. 20036

SUBJECT: Structural Loads Induced by AAP
Spacecraft Docking Dynamics
Case 620

DATE: April 1, 1968

FROM: W. W. Hough

MEMORANDUM FOR FILE

INTRODUCTION

Analyses of structural loads induced in the AAP Cluster by spacecraft docking dynamics are being performed by both the Structures and Mechanics Division at the Manned Spacecraft Center and by the Martin Company, who is under contract to the Marshall Space Flight Center. The bending moment at the established LM-ATM/MDA interface (MDA port 1) which is induced when the CSM docks to the axial MDA port (port 5) is the particular load that has received the most attention. The maximum moment calculated by MSC is a factor-of-five greater than the value found by Martin for the same set of initial conditions. Acceptance of the MSC value as the design limit load implies redesign of the LM ascent stage structure and a relatively heavy MDA structure, while a value 30-40% less is within present structural capabilities.

MSC and Martin use the same basic technique in their loads analyses. Time-histories of probe/drogue contact loads are generated by MSC with a rigid-body docking dynamics program. These loads are then applied by both MSC and Martin as forcing functions in elastic body response programs that model the Cluster. The difference between the MSC and Martin results is due solely to differences in the mathematical models of the Cluster used in the respective response analyses. The primary influence is the stiffness model of the LM/MDA interface.

In this memorandum, LM/MDA interface bending moment is examined as a function of that interface stiffness. Two approaches are used in the analysis of a simplified model. The results from a two-step approach of the type used by MSC and Martin are compared with the results from a combined (one-step) analysis. The one-step approach includes the effect on probe loads and frequencies of docking elastic rather than rigid bodies.

It must be understood from the outset that the results obtained from these analyses are not intended for use in structural design. The intent is to examine the trend of bending moment vs. interface stiffness and give insight into the conservatism or optimism of the two-step approach used in the detailed analyses of Martin and MSC.

PARAMETRIC ANALYSES

Figure 1 schematically shows the two-step approach used by MSC and Martin. It also depicts the model used in the simplified analysis presented here. In the first step of the simplified two-dimensional analysis, the determination of probe load-time histories begins as the probe head of the chase vehicle engages the drogue apex on the target vehicle at point P. This point is maintained as a pinned joint with no rotational restraint throughout the problem. The model of the probe consists of axial and lateral linear springs, K_A and K_L , and parallel viscous dampers. Four initial conditions are required to determine deflections of the springs. These are the relative velocities in the x and y directions, the relative angular rate, and the initial angle between the centerlines of the vehicles.

MSC's detailed program for determination of the probe loads solves the three dimensional problem. Loads that occur before capture of the probe head because of initial lateral offsets are determined. Ten initial conditions are required. These are relative velocities in three directions, angular positions and rates about the y and z axes, index angle, and the initial offsets in the y and z directions. The model of the probe is accurate; it includes the non-linear characteristics of stiffness and damping. The computer program has been checked in a scale model test program as well as with full-scale mechanism tests. The outputs of the program are the time-histories of three forces and three moments at the center of the drogue/MDA attachment plane. The outputs of the first step of the simplified analysis are the time histories of the axial and lateral forces, $F_x(t)$ and $F_y(t)$.

The second step in the two-step approach is to apply the load-time histories in an elastic body response analysis. In the simplified analysis, a four degree-of-freedom model is employed (3 rigid-body modes and one elastic mode). Bending moment at the LM/MDA interface is determined by multiplying the deflection of the bending spring, K_α , by its stiffness. In the detailed Martin analysis, a model with six rigid-body modes and over 80 elastic modes is employed. The results of the simplified analysis are comparable with the results of the detailed analysis because motion in the lower elastic modes is primarily bending (in two directions) at the interface. As these lower modes are the prime contributors in the total response, the model with only one elastic mode is an excellent approximation in the two dimensional problem.

Figure 2 depicts the model used in the combined, or one-step analysis. Because of the simplicity of the model, combination of the two steps adds only one elastic degree of freedom to the first step of the other approach. There are seven degrees of freedom and therefore seven modes: three elastic modes and four with zero frequency. The fourth mode with no elastic contribution is due to the pinned joint at P.

The one-step approach will yield a more accurate solution for loads induced after the capture-latch event, as it includes the effect of docking to an elastic rather than a rigid body.

RESULTS OF SIMPLIFIED ANALYSIS

Both the one-step and the two-step approaches were used to determine time-histories of probe forces and LM/MDA bending moments over a four-order-of-magnitude range of LM/MDA interface stiffness, K_α . The same set of four initial conditions was used in each case:

$$\begin{aligned} \text{Relative Closing Velocity} &= -\dot{\Delta}_{x0} = 1 \text{ ft/sec} \\ \text{Relative Lateral Velocity} &= \dot{\Delta}_{y0} = -0.5 \text{ ft/sec} \\ \text{Relative Initial Angle} &= \theta_{c0} = -10^\circ \\ \text{Relative Initial Rate} &= \dot{\theta}_{c0} = 1^\circ/\text{sec} \end{aligned}$$

In this set, all values are at a maximum limit of the Apollo initial-condition envelope, but the combination does not necessarily produce the worst bending moment for any value of K_α used. The stiffness of the LM/MDA interface was varied from $K_\alpha = 10^5$ ft. lb./radian to $K_\alpha = 10^9$ ft. lb./radian.

Figure 3 gives an example probe axial load history from the one-step analysis (time zero = capture-latch event). This particular plot is for $K_\alpha = 6 \times 10^6$ ft. lb./radian.

Figure 4 gives the history of probe lateral force for the same case. Comparable plots from the first step of the two-step analysis are independent of K_α , and approximate pure damped sinusoids. Figure 5 is a plot of the LM/MDA bending moment for

the case of $K_\alpha = 6 \times 10^6$ ft. lb./radian from the one-step analysis. The history of the bending moment from the second step of the two-step analysis for the same K_α is similar in shape.

Figure 6 presents a comparison of the three normal elastic mode frequencies that are obtained in both approaches. Frequencies are plotted against the stiffness parameter, K_α .

The horizontal dashed lines are the natural frequencies of the probe and rigid vehicle system analyzed in the first step of the two-step approach. The frequency of the probe axial mode (.81 cps) and the probe lateral mode (2.2 cps) are independent of the stiffness parameter. The dashed sloping line is the elastic mode frequency associated with the LM/MDA bending. This frequency is a property of the model used in the second step of the two-step approach, and is proportional to the square-root of the stiffness parameter. (This characteristic is shown by a straight line with a slope of 1/2 on a log-log plot). Two values of the stiffness parameter exist where the response frequency is identical to a probe forcing frequency. With the two-step analysis, a perfectly tuned or resonant condition can exist.

The three solid lines are the frequencies of the three elastic modes derived from the one-step analysis. They do not cross; in the stiffness region where the two-step approach gave resonant conditions, the characteristics of the mode shapes change. For example, in the stiffness region below 10^6 ft. lb./radian, the first mode is primarily interface bending, the second is primarily probe axial motion, and the third is primarily probe lateral motion. But at a stiffness value of 10^7 ft. lb./radian, the first mode becomes primarily probe axial motion, and the second mode becomes primarily interface bending. In the region 3×10^6 to 4×10^6 ft. lb./radian, it is impossible to describe either the first or second mode shapes as primarily motion of one of these springs. The point to be made is that it is impossible to achieve a perfectly tuned condition after the capture latch event.

Figure 7 shows the peak probe axial forces determined in both analyses vs. the stiffness parameter. Figure 8 is a similar plot of the peak probe lateral loads. The dashed lines were obtained in the first step of the two-step approach, and are independent of K_α . The solid lines show the results of the one-step analysis. With an infinite K_α , the solid and dashed lines must meet.

The maximum bending moments at the LM/MDA interface are plotted vs. the stiffness parameter in Figure 9. The dashed line was derived from the second step of the two-step approach. Damped sinusoidal forcing functions were applied to the elastic model in the x and y directions at point P. The solid line was derived from the one-step analysis. At stiffness values of the LM/MDA stiffness below 6×10^6 ft. lb./radian, the results obtained by the two-step analysis are shown to be conservative. While a peak bending moment of about 520,000 inch pounds is obtained when the frequency of the bending mode is equal to the axial probe driving frequency, the more accurate analysis (in which a tuned condition cannot occur) yields a maximum of about 410,000 inch pounds.

DISCUSSION AND CONCLUSIONS

The reason for the factor-of-five difference in maximum bending moments calculated by MSC and Martin is illustrated by Figure 9. Their elastic models differed in the stiffness of the LM/MDA interface. The stiffness in the Martin model resulted in a maximum moment of about 100,000 inch pounds (equivalent to a stiffness of 8×10^5 ft. lb./radian in the simplified two-step analysis), while the stiffness of the MSC model was somewhat greater (over 4×10^6 ft. lb./radian), and resulted in the tuned response condition.

Based on the results of this analysis, some tentative conclusions can be drawn. MSC does not agree with all of these conclusions for reasons that will be pointed out.

1. The bending moment can be kept within the existing structural capability of the LM ascent stage by keeping the interface stiffness either lower or higher than the values that result in (approximately) tuned conditions. If it is kept lower, the MDA weight will be minimized, whereas substantial weight penalties will result if it is made higher.
2. With an interface stiffness lower than that which produces a tuned condition, the driving and response frequencies can be further separated by increasing the stiffness of the probe. There is a very simple mechanical means of accomplishing this; the Belleville washers in the probe support struts can be stacked in a different fashion, and this can be done late in the program.

3. A more accurate one-step analysis will give lower values of bending moment than those presently obtained in the two-step approach within the lower region of interface stiffness.

MSC's objections are based on what might happen before the capture latch event due to initial lateral offsets. Their studies have shown that the probe head can bounce from side-to-side within the drogue before capture. The frequency of these impulsive-type loads is heavily dependent on initial conditions as well as on probe stiffness. These recurring impulsive loads could excite the interface bending modes. MSC points out that excitation of low frequency modes is likely to be more damaging than excitation of high frequency modes. For this type of load, the difference between the one and two-step approaches will probably not be as great as indicated in the simplified analysis presented here.

STATUS

MSFC has decided to design the MDA ports for a limit load capability approximately equivalent to the load carrying capability of the Apollo modules (300,000 inch pounds). A factor-of-safety of 1.4 will be used (i.e., the ultimate load capability will be 420,000 inch pounds). This configuration will weigh about 400 pounds less than the previous configuration which was designed for a 500,000 inch pound limit load. When elastic models for the final configurations are agreed to by the Centers, MSC will run a final loads study. This entails searching the range of initial conditions for critical cases. If their fears concerning the low MDA stiffness are realized (neither MSFC or the author expect that they will), the probe stiffness modification can be incorporated. If this modification does not completely eliminate the problem, the initial condition envelop of CSM/MDA relative velocities can be tightened. Apollo has investigated possible changes to the envelope to reduce probe mechanism loads, and has concluded that reductions in both axial and lateral closing-velocity limits are feasible.

In summary, MSFC expects the more flexible MDA design will eliminate the bending problem. If they are wrong, there are two other means that can be employed to eliminate the problem, both of which are simple to implement. The weight saving that results from their decision to build the more flexible configuration is about 400 pounds.

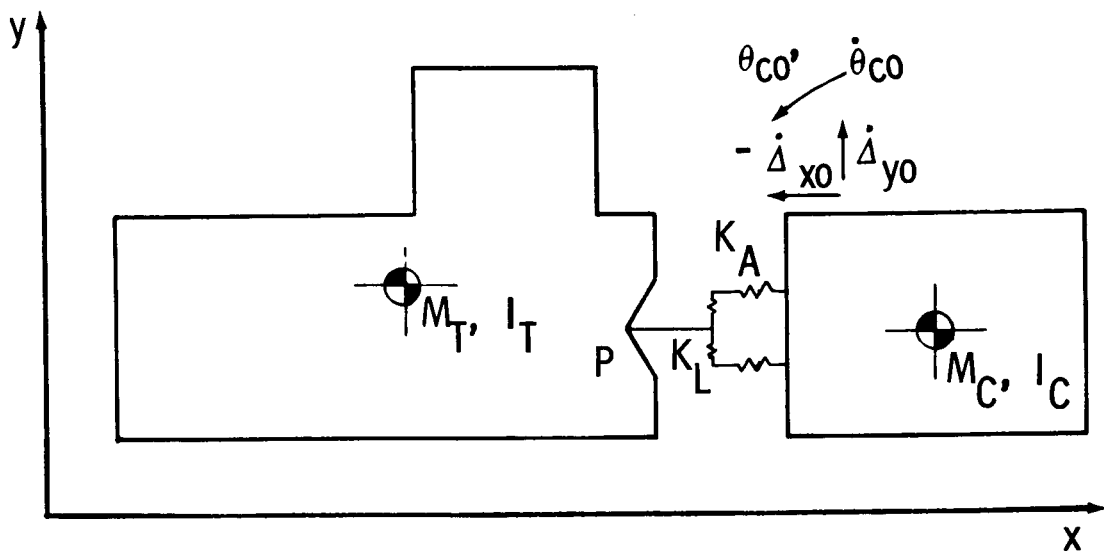


W. W. Hough

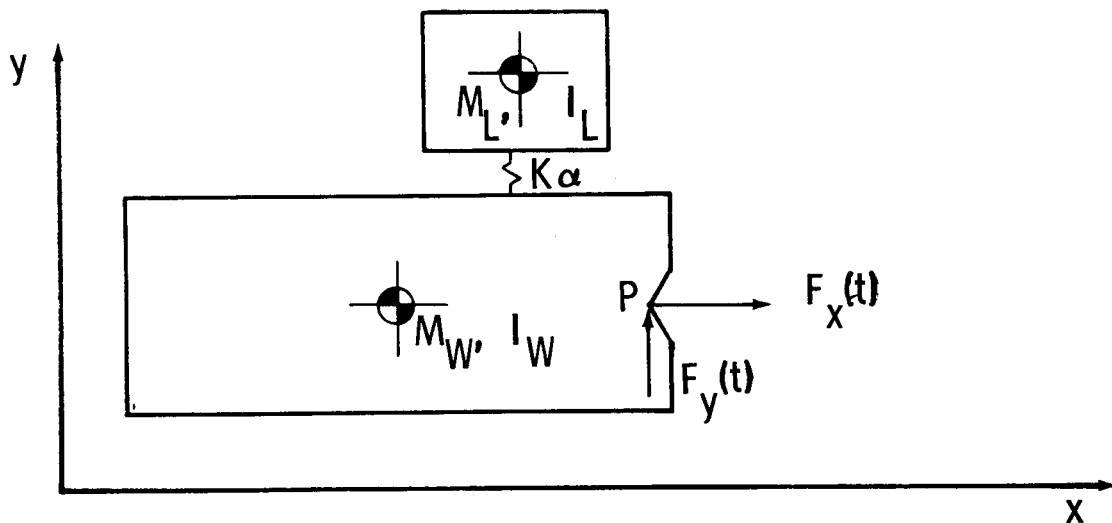
1022-WWH-mef

Attachments

Figures 1-9



STEP 1: CALCULATE LOAD-TIME HISTORIES AT PROBE/DROGUE INTERFACE FROM IMPACT OF TWO RIGID BODIES WITH MODEL OF PROBE BETWEEN



STEP 2: APPLY LOADS FROM STEP 1 TO ELASTIC RESPONSE ANALYSIS OF WORKSHOP/LM-ATM COMBINATION TO DETERMINE LM/MDA INTERFACE LOADS

FIGURE 1 - TWO-STEP APPROACH USED BY MSC & MARTIN

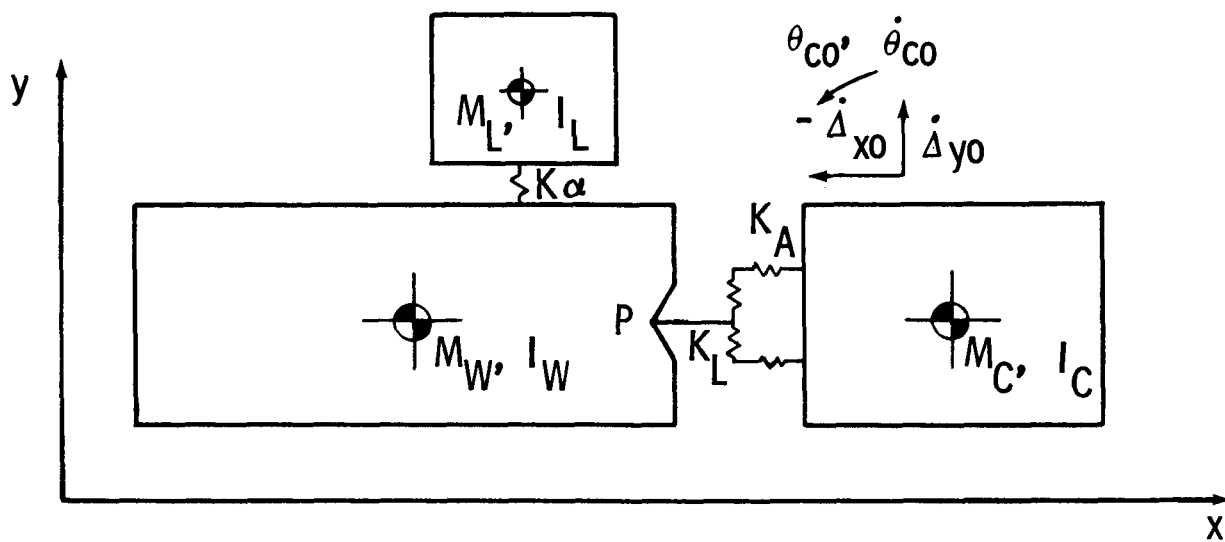


FIGURE 2 - ONE-STEP APPROACH

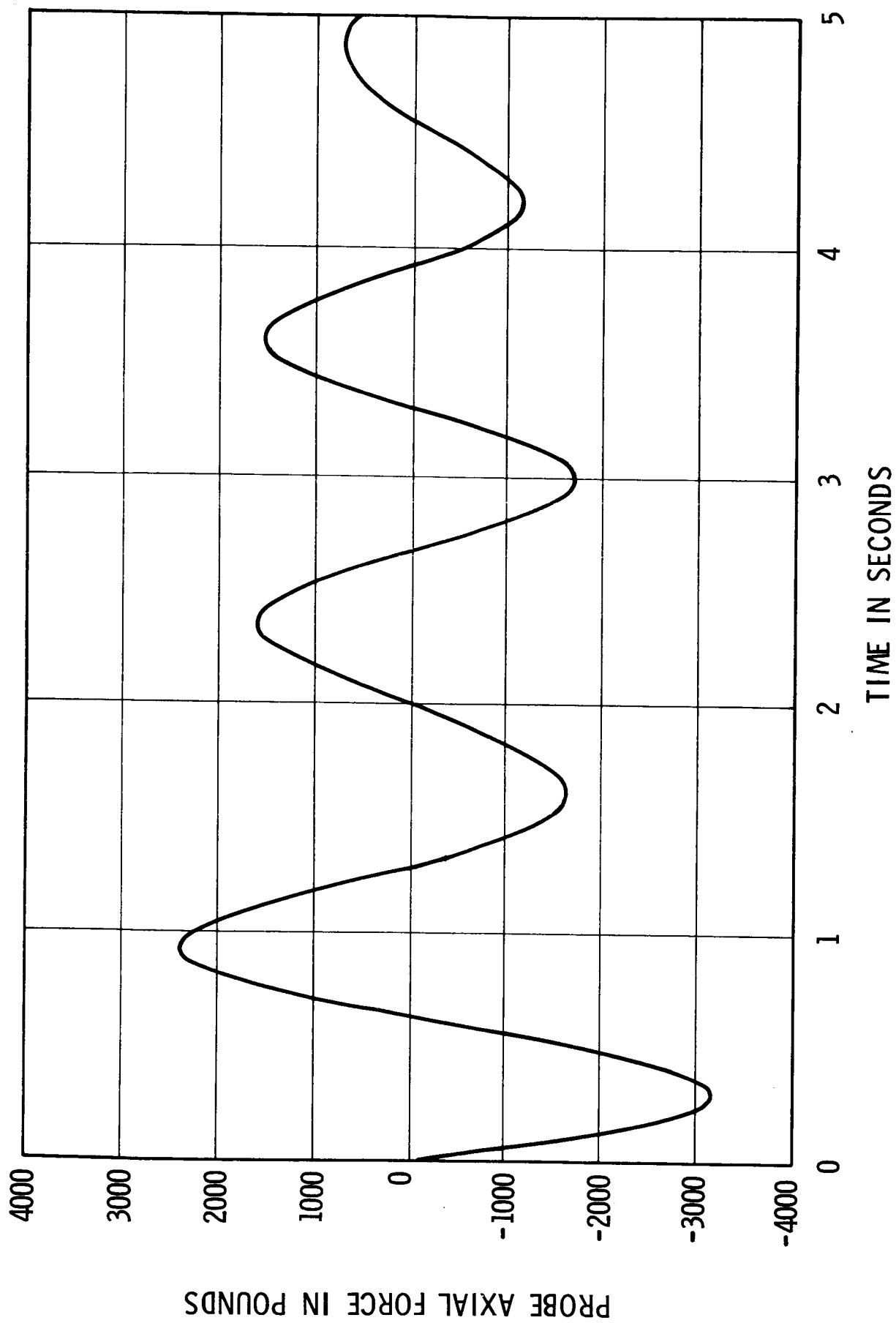


FIGURE 3 - TIME HISTORY OF PROBE AXIAL LOAD

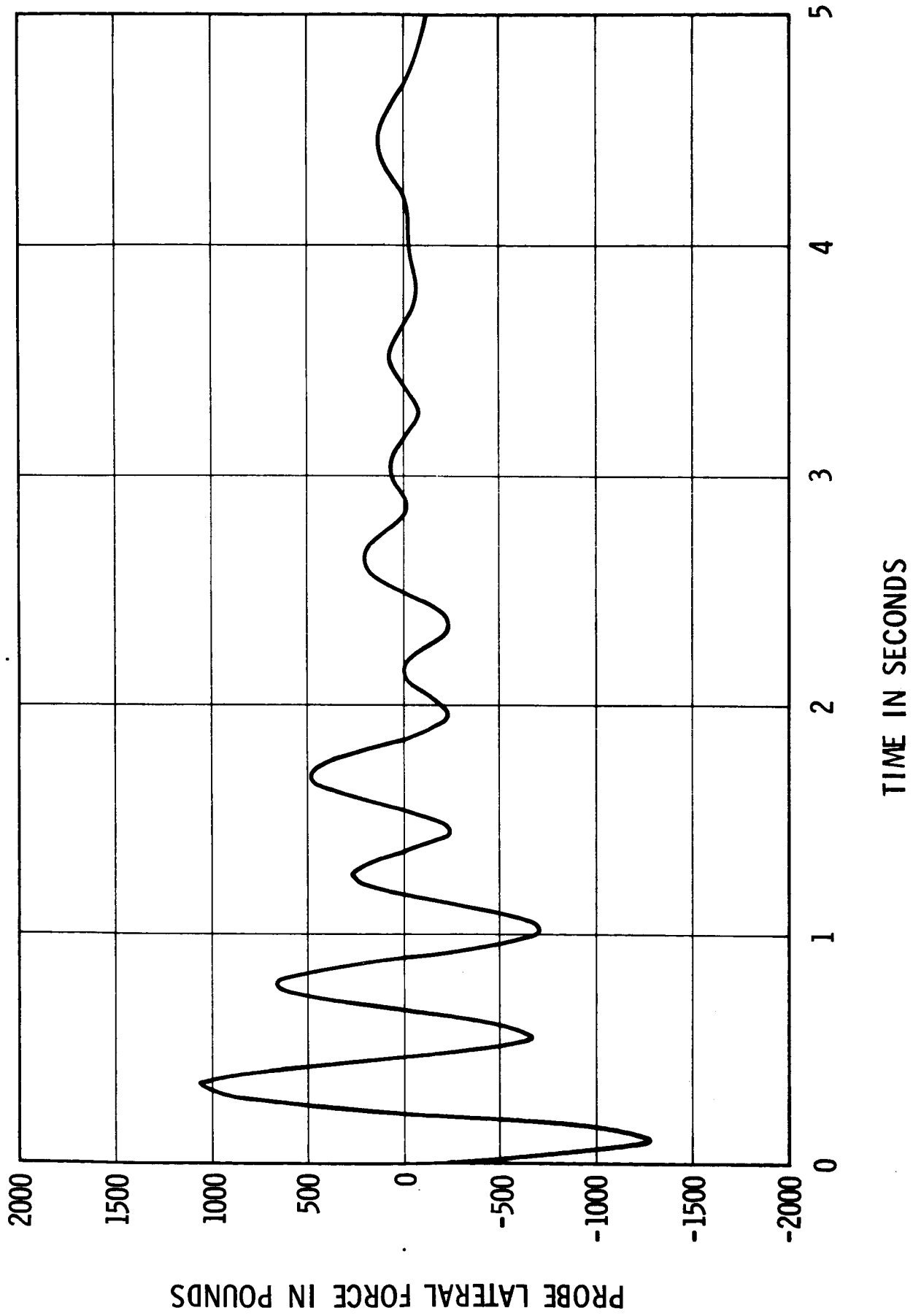


FIGURE 4 - TIME HISTORY OF PROBE LATERAL LOAD

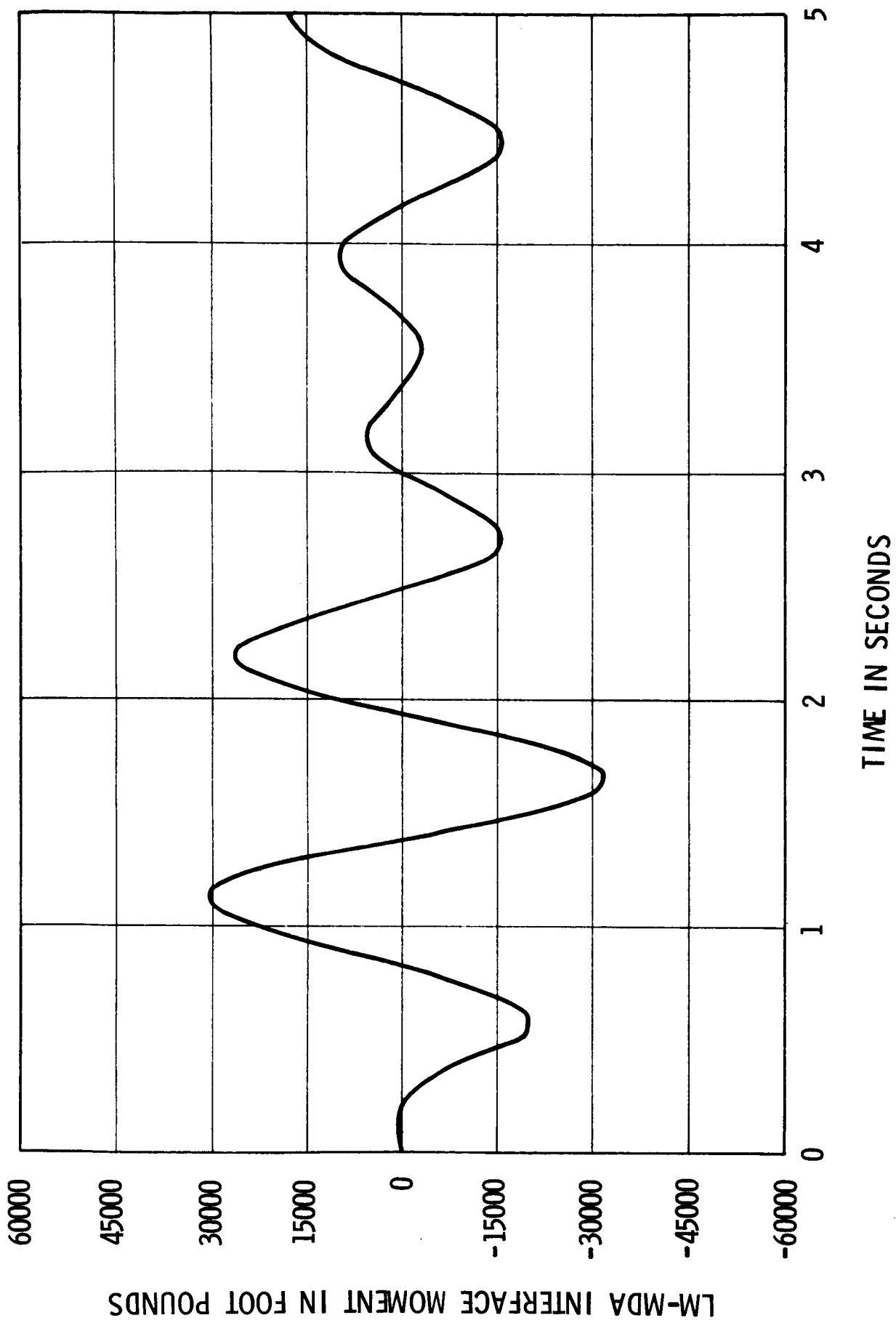


FIGURE 5 - TIME HISTORY OF LM/MDA INTERFACE MOMENT

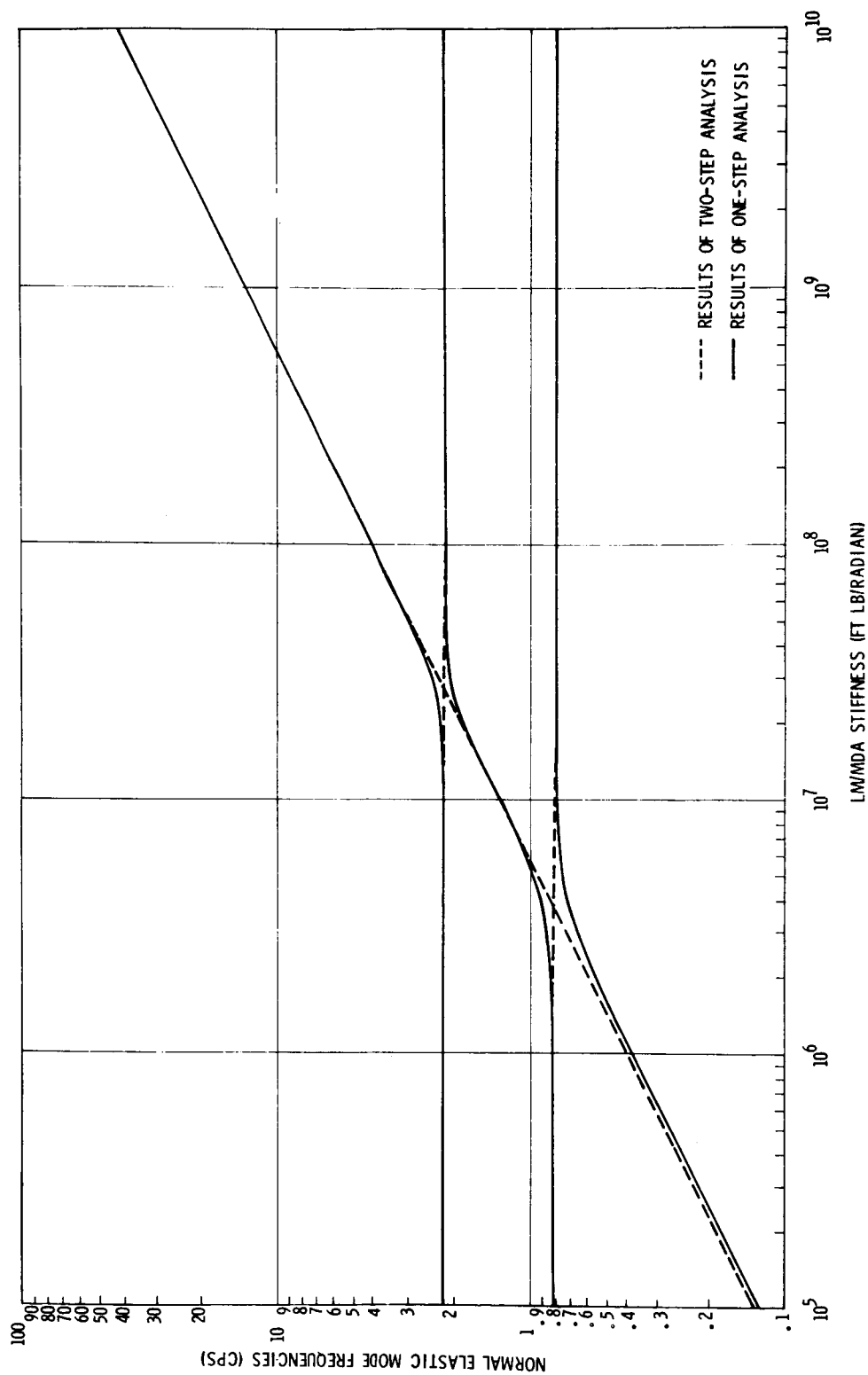


FIGURE 6 - NORMAL ELASTIC MODE FREQUENCIES vs. LM/MDA STIFFNESS

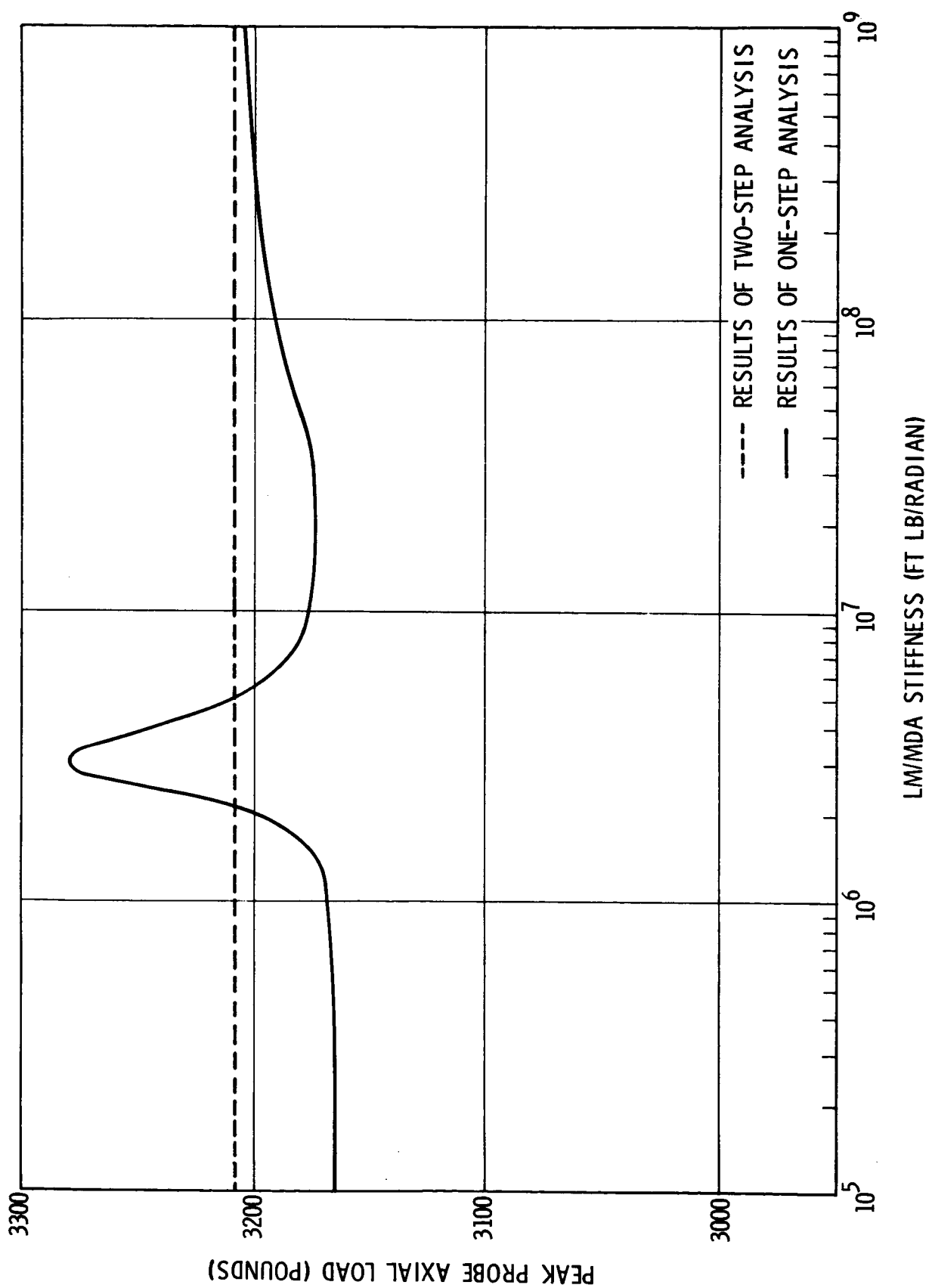


FIGURE 7 - PEAK PROBE AXIAL FORCE VS. LM/MDA STIFFNESS

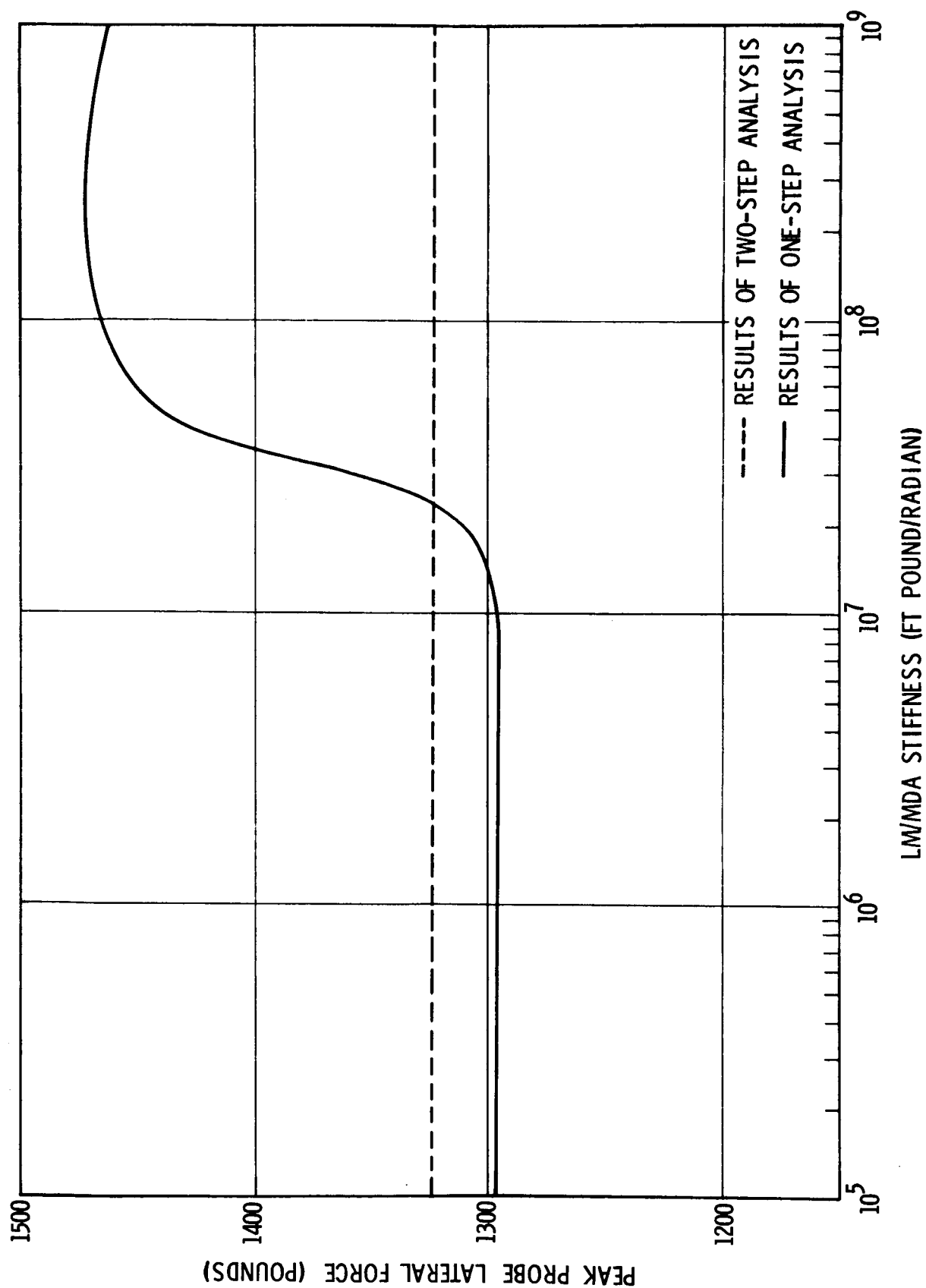


FIGURE 8 - PEAK PROBE LATERAL FORCE vs. LM/MDA STIFFNESS

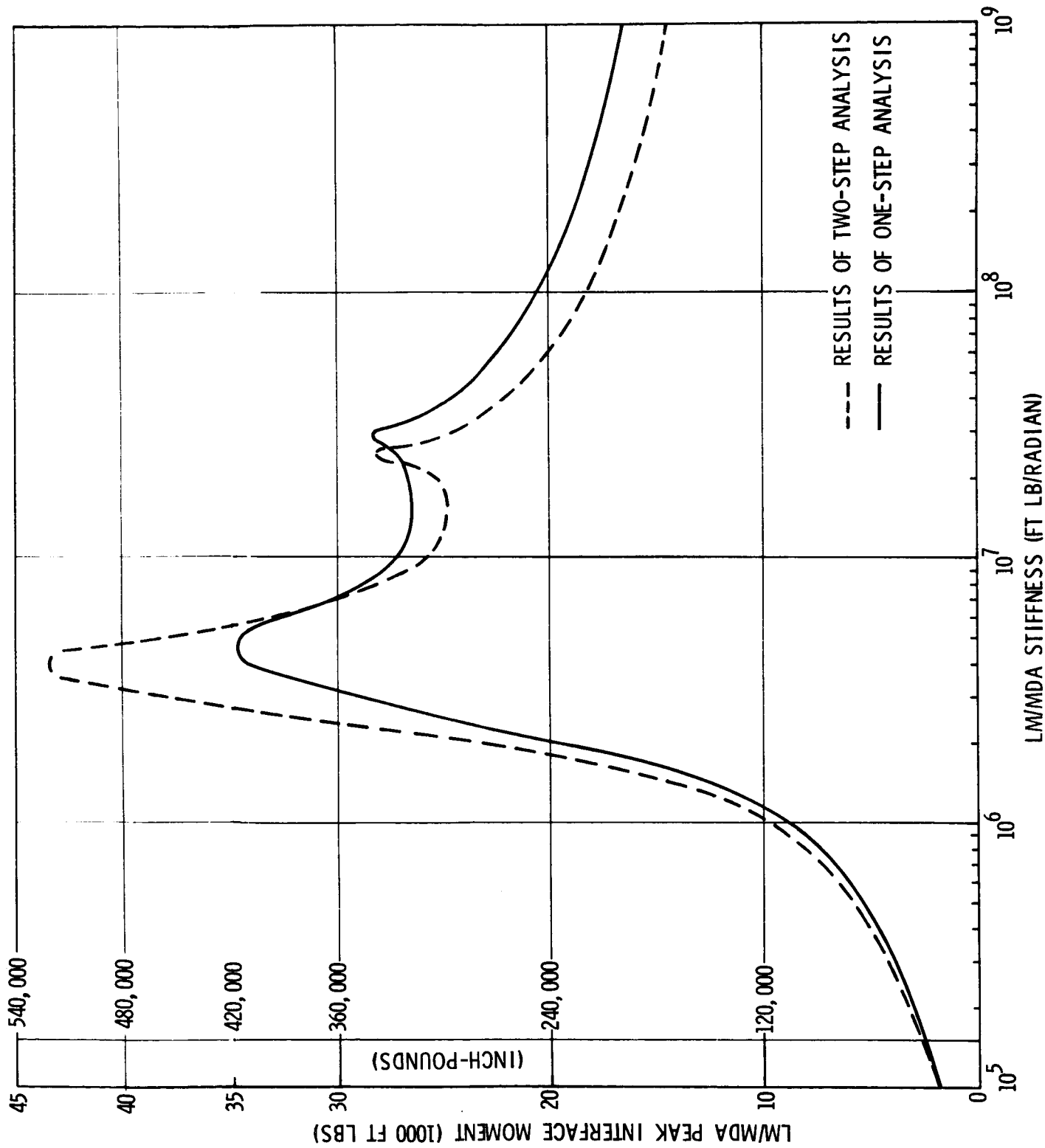


FIGURE 9 - PEAK INTERFACE MOMENT vs. LM/MDA STIFFNESS

BELLCOMM, INC.

Subject: Structural Loads Induced by AAP From: W. W. Hough
Spacecraft Docking Dynamics

Distribution List

NASA Headquarters

Messrs. E. P. Andrews/MLA
H. Cohen/MLR
P. E. Culbertson/MLA
J. H. Disher/MLD
J. A. Edwards/MLO
L. K. Fero/MLV
J. P. Field, Jr./MLP
T. A. Keegan/MA-2
H. Mannheimer/MLA
C. W. Mathews/ML
M. Savage/MLT

MSC

Messrs.	J. Barneburg/ES-2	W. B. Evans/KM
	L. A. Bernardi/KS	R. M. Machell/KF
	H. W. Dotts/KS	D. C. Wade/ES-2

MSFC

Messrs.	E. E. Beam/R-P&VE-SL	G. B. Hardy/I-S/AA
	T. Bullock/R-P&VE-SLR	W. B. Holland/R-P&VE-SLR
	G. Eudy/R-P&VE-E	H. R. Palaoro/R-P&VE-SL

Bellcomm

Messrs.	A. P. Boysen	Div. 101 Supervision
	D. R. Hagner	Div. 103
	B. T. Howard	Dept. 2015 Supervision
	J. Z. Menard	All Members Dept. 1021, 1022, 1024, 1025
	I. M. Ross	Department 1023
	R. L. Wagner	Central File
		Library